Arch. Min. Sci. **69** (2024), 3, 431-446

Electronic version (in color) of this paper is available: http://mining.archives.pl

DOI: https://doi.org/10.24425/ams.2024.151444

JAN BLACHOWSKI[1], JAROSŁAW WAJS[1*],
NATALIA WALERYSIAK[1], MIŁOSZ BECKER[2]

MONITORING OF POST-MINING SUBSIDENCE USING AIRBORNE AND TERRESTRIAL LASER SCANNING APPROACH

Discontinuous deformations, such as sinkholes, pose significant challenges in post-mining areas due to their unpredictable nature and potential hazard to surface development and the safety of local communities. Therefore, monitoring the post-mining regions should be treated as a continuing task. This study addresses the ongoing problem of sinkhole formation in the former "Przyjaźń Narodów – Szyb Babina" (Babina) lignite mine located in the glaciotectonic region of Muskau Arch in western Poland. The research uses airborne and terrestrial laser scanning methods to identify and monitor discontinuous deformations, focusing on a newly discovered sinkhole. The methodology involves differential analysis of Digital Elevation Models (DEMs) and their derivatives obtained from airborne laser scanning (ALS) and periodic terrestrial laser scanning (TLS) measurements. The results of ALS DEM analysis allowed the successful identification of 75 confirmed sinkholes, the largest measuring 12.8 m in diameter and 4.8 m deep. Whereas, differential DEM analysis indicated new sinkholes that developed between 2011 and 2020 in the area of shallow underground mining. Two-year TLS monitoring of the new sinkhole showed no progression in its dimensions. However, localised erosion processes associated with water transport were detected. The study shows that sinkhole formation processes are active 5 decades after the end of mining and highlights the importance of continuous monitoring of post-mining areas with advanced laser scanning methodss.

Keywords: Sinkholes; post-mining; lignite; monitoring; TLS; ALS; geopark

1. Introduction

Discontinuous deformations such as sinkholes are one of the potential, undesirable, difficult-to-predict, and hazardous phenomena associated with underground mining. Sinkholes can occur

[1] WROCLAW UNIVERSITY OF TECHNOLOGY, WYBRZEZE WYSPIANSKIEGO 27, 50-421, WROCLAW, POLAND
[2] KGHM CUPRUM SP. Z.O.O. – RESEARCH AND DEVELOPMENT CENTRE

* Corresponding author: jaroslaw.wajs@pwr.edu.pl

in post-mining areas decades after the termination of mining operations [1-3]. The sinkhole development mechanism is related to cavities developing in the subsurface caused by the overlying strata moving into underground excavations due to deterioration of roof support. Gradually, these movements continue to the surface, in the form of a chimney, and a depression forms on the ground surface. Shallow underground mining operations, up to 100 m below ground surface, abandoned without proper liquidation measures, are particularly susceptible [4]. Surface cave-ins 2 m wide and up to 17 m deep have been observed over shallow lignite workings leading to open chimneys [5]. Tajduś et al. [6], based on a detailed analysis of case studies, have highlighted the lack of detailed knowledge about the locations of old underground mine workings, including shafts and drifts, and their current conditions, as the primary reasons for ineffective subsidence risk management. Predicting discontinuous deformations such as sinkholes involves mainly analysing the conditions conducive to their formation and development [7]. Sinkhole risk research includes among other things: geophysical measurements of the rock mass to detect voids and remnants of underground mining activity [8-10], analysis of archival cartographic materials documenting extraction of minerals from deposits [11-13], setting up systems such as stations and networks for recording microseismicity [14], developing various risk assessment models based on machine learning assumptions, analytical hierarchy process analysis, weight of evidence, rock mass pressure theories, that are designed to identify areas at risk of discontinuous deformations [15-18]. An example of sinkhole occurrence information and prevention measures is the Upper Silesian Surface Hazard Information System for Decommissioned Mines, available at https://zapadliska.gig.eu/ [19]. The service provides information on the location of shallow coal and metal ore mining areas in the Upper Silesian Coal Basin (GZW).

Due to the localised nature of subsidence formation in mining areas and karst regions, geodetic techniques such as precise levelling and terrestrial laser scanning (TLS) are the most commonly used for terrain movement monitoring [20-21]. Low-altitude photogrammetry is also used under favourable terrain coverage conditions. For example, [22] used Unmanned Aerial Vehicle (UAV) to register images for constructing a digital terrain model (DTM) with 5 cm spatial resolution and 14 cm vertical accuracy, which was considered acceptable for subsidence mapping purposes, and [23] tested UAV photogrammetry and LiDAR data for detection and measurement of terrain deformations caused by underground mining regarding TLS data. The authors determined that the UAV photogrammetry provided more accurate results of the terrain subsidence measurement than the unmanned aerial system (UAS) LiDAR sensors for a test site in an underground hard coal mining area. There are also studies describing the use of satellite radar interferometry (InSAR) for monitoring and predicting such subsidence events in karst areas in Italy [24] and in mining areas in Turkey [25]. Authors of [26] successfully identified 11 sinkholes in mining areas in Poland with a maximum depth of 16 m using Persistent Scatterer Interferometry (PSI) and indicated that the density of coherent points should be higher than 1 point per 30,000 m^2. However, applications of airborne and satellite methods are limited in vegetated and woodland areas.

Numerous cases of discontinuous deformations occurring in post-mining areas and causing destruction on the surface, such as recently in the former "Siersza" coal mining area in SW Poland [27], indicate that monitoring and predicting sinkhole occurrence remains a current research problem.

This article presents the results of research aimed at identification and monitoring of discontinuous deformations using modern airborne and terrestrial laser scanning methods. The specific objective was to assess if there is a development in the dimensions of the newly identified sinkhole.

The research focused on the “Pustków” mining field of the old “Przyjaźń Narodów – Szyb Babina” (Babina) lignite mine in the Lubuskie Voivodeship, western Poland, where new subsidence events continue to occur five decades after the end of mining. The study area is shown in Fig. 1.

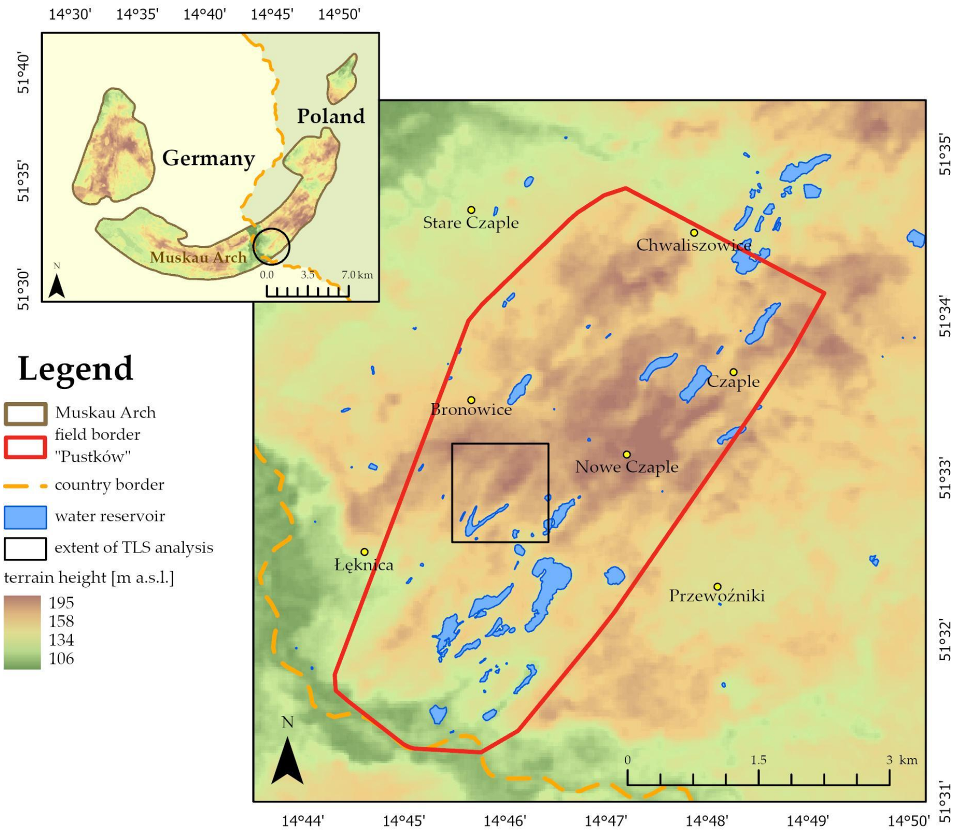

Fig. 1. Boundaries of the “Pustków” mining field in the “Przyjaźń Narodów – Szyb Babina” mine and the study area (black box)

2. Study area

The lignite mine “Przyjaźń Narodów – Szyb Babina” operated within the eastern part of the glaciotectonic structure known as the Muskau (Mużaków) Arch from 1921 to 1973. The arch is a terminal moraine of horseshoe shape open to the north [28] and its eastern arm lies between the localities of Łęknica and Tuplice in Poland. It is made of parallel, elongated, hills, which have a maximum width of 6 km and relative heights of 20-30 m. The moraine is separated into two symmetrical parts by the Lusatian Neisse (Nysa Łużycka) river, the western one in Germany and the eastern one in Poland [29].

Glaciotectonic processes deeply disturbed originally horizontal lignite deposits in the area. Mining of the resulting steeply inclined coal seams was carried out using underground (initially) and open-pit (in the later stages) methods. Shallow underground mining utilised the room and pillar mining system and because of the inclination of lignite deposits the mining levels were developed in a stepped manner, descending downward. The levels were connected by drifts used for transporting coal to lower galleries and to the main haulage level. To access the underground mine from the surface inclined access tunnels were constructed owing to the shallow depth of the lignite deposits that ranged from several to about 100 m below the ground level [30]. Underground mining produced distinctive deformations of the terrain surface in the form of longitudinal subsidence troughs and sinkholes. The subsidence troughs emerged above the galleries shortly after mining began. There are two types of troughs in the topography. The first category is characterised by widths of up to several tens of meters and lengths of 2 to 3 km. Inside these forms, there are numerous distinctive and frequently evenly distributed sinkholes. These are usually situated above former underground voids. The sinkholes are typically 2 to 4 m in diameter and in depth. The second type of troughs have a more irregular shape with lengths of several hundred meters and variable widths that range from 50 to 150 m. The shape of these forms, usually several meters deep and sometimes filled with water, is related to the inclination of coal seams and the distribution of underground workings [31]. Additionally, larger sinkholes of spherical shape and greater depth developed above former shafts (e.g., ventilation shafts) and access tunnels.

2.1. State of knowledge on mining deformations in the Muskau Arch area

Previous studies in the post-mining area near the town of Łęknica have predominantly focused on assessing the state of the environment, specifically the state of vegetation and soil in reclaimed areas. [32-34], and assessment of the water quality in anthropogenic reservoirs (former open-pits) [35-37].

The problem of surface deformations, particularly of a discontinuous nature, and protecting the area has not yet been resolved despite the appearance of new sinkholes. Efforts have only been made to record existing damages [38]. Other studies include research of significant anthropogenic transformation of the land's surface linked to open-cast and underground mining in the analysed part of the Łuk Mużakowa region were presented by Koźma and Kupetz [28] and Koźma [31]. These studies utilised archival cartographic materials (German and Polish topographic maps), aerial imagery, and digital elevation models (DEM) for quantitative analysis of anthropogenic landforms. Analysis of historical mining activity in the Zielona Góra region north of the study area was presented by Gontaszewska [13], and the general conditions of the occurrence of post-mining damage related to lignite mining in the Lubuskie region have been described in Gontaszewska [30].

On the German side of the Muskau Arch, Munch and Nestler [39] conducted an analysis of the potential hazards resulting from past underground mining activities, using data from aerial laser scanning and orthophotos. The authors indicated the potential of DEM data, in addition to archival mining maps, for estimating the extent of underground mining especially in densely vegetated areas.

The National Science Centre OPUS-17 and OPUS-22 projects "Genesis and course of anthropogenic and natural deformations of the terrain in post-mining areas of the former brown coal mine "Babina", stages 1 and 2 (number 019/33/B/ST10/02975 and 2021/43/B/ST10/02157) are the first comprehensive studies on post-mining transformations on the Polish side. In the following sections selected results from these projects concerning research on sinkhole monitoring are presented.

3. Methodology

Various techniques are available to identify transformations occurring in the topography, particularly in sinkhole-prone areas [40]. One of the frequently utilised methods is to compare Digital Elevation Models (DEMs), commonly known as DEM of Difference (DoD) [41]. In the raster analysis approach the data for comparing models can be acquired with photogrammetric techniques [42] or LiDAR measurements. Active LiDAR sensors have the advantage of detecting ground movements of the surface that is covered by vegetation [43]. To generate digital elevation difference models, the data can be processed through point-to-point [44], point-to-continuous surface TIN-MESH [45], or point-to-model [46] analysis. In the process, the accurate and precise georeferencing of LiDAR data is essential. It is achieved using fixed reference points (Ground Control Points, GCP), whose coordinates are acquired using a reliable, independent measurement technique, such as the Global Navigation Satellite System (GNSS) [47].

In this study, a two-stage methodology for identifying and monitoring discontinuous deformations is proposed and tested in the Muskau Arch study area. The first stage involves differential analysis of Digital Elevation Models (DEMs) constructed from publicly available aerial laser scanning (ALS) data acquired in 2011 and 2020. In the second one, monitoring of a newly identified sinkhole is conducted by comparing DEMs developed based on terrestrial laser scanning (TLS) data, acquired periodically between 2020 to 2022. The digital encoding of archival mining maps, drawn at a 1:10,000 scale between 1956 and 1973 to assist the analysis accompanied these activities. The maps were obtained from the archive of the Higher Mining Office and encoded using ESRI ArcGIS Pro 2.9 software licensed to the Wrocław University of Science and Technology.

3.1. Identification of ground movement with Aerial Laser Scanning data

Data from aerial laser scanning commissioned by the Head Office of Geodesy and Cartography carried out in April 2011 and April 2020 are represented by point clouds with 4 point/m^2 spatial resolution. Each point is defined by its horizontal coordinates and a vertical coordinate with an accuracy of mdh $\leq$ 0.15 m. In the initial analysis, points classified as "ground" representing the terrain surface free from vegetation were used to construct Digital Elevation Models with a resolution of 0.5 m. Then, the local map algebra function was used to subtract values of spatially congruent raster cells to develop a differential DEM.

A processing model was constructed to identify elevation changes over the examined period. The model identifies clusters of pixels with differences in values (heights) greater than 0.5 and 1.0 m. Additionally, derivative DEMs representing slope and shaded relief surfaces were calculated to assist identification of discontinuous deformations and subsidence troughs.

3.2. Monitoring of sinkholes with Terrestrial Laser Scanning data

This part of the research involved three main steps presented below.

3.2.1. Establishment of ground control points

A network of 7 measurement points was set up as a georeferencing control for the point cloud data. Due to the characteristics of the study site, 3 control points – TLS stations – were established in a wooded area of the study site and additional, 4 reference points were set up outside of the wooded zone. The location of the measured points on the ortophotomosaic and a scheme of the survey line is presented in Fig. 2. The control points outside of the wooded site were measured independently using the static GNSS technique and the entire control network was surveyed using geodetic traverse and precise levelling regarding 2 higher-class benchmarks. The adopted design of the control network enabled precise georeferencing of the point clouds collected from 3 stations.

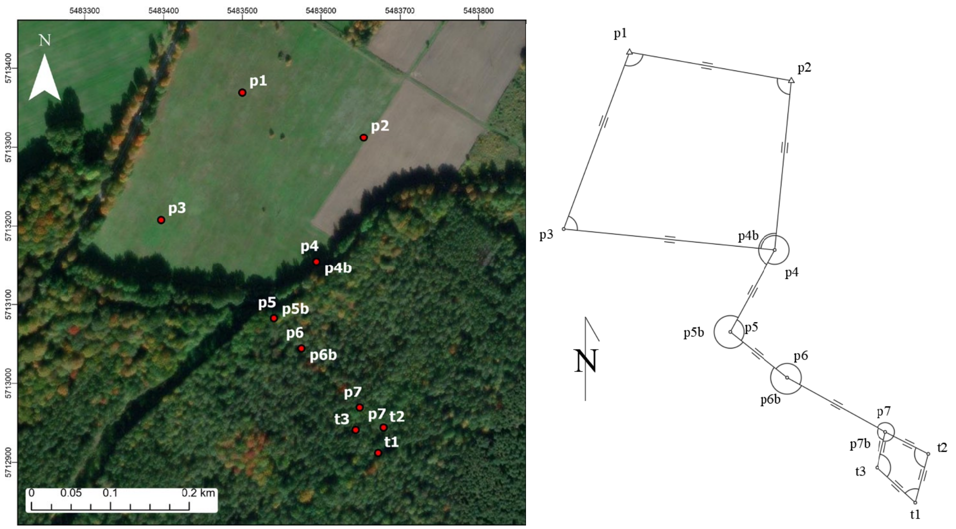

(a) (b)

Fig. 2. Location of surveying grid points on the background of orthophotomosiac (a), sketch of polygon sequence (b)

3.2.2. Terrestrial Laser Scanning

The TLS measurements were conducted using the Riegl VZ-400i laser scanner and a 360° panoramic method of observations, enabling the acquisition of data in all directions from the sensor position. Due to the sinkhole shape and the danger of ground collapse under the weight of a person operating the scanner, measurement locations were positioned about 3-5 m from the edge of the analysed feature. The sphere of vision of a laser scanner mounted vertically on a tripod is limited to 100° [48] and the measurements cannot be performed directly above or below the scanner head.

The stop-and-go technique with a step of approx. 5 m concerning three control points positioned outside of the sinkhole's immediate influence was used to acquire point cloud data. Terrestrial laser scanning was done using a predefined panoramic scan profile – panorama 40 with a scanning resolution of 360 degrees at 40 mdeg intervals. A single scanning station allowed for the registration of approximately 10 million points and identification of reference targets with 150 mm diameter, mounted on two-metre poles with bipods. A GNSS receiver was attached to the scanner head during TLS measurements and the registered point cloud was assigned initial coordinates in the global WGS84 coordinate system. However, precise GNSS-fix solutions were not possible due to the presence of trees in the analysed area. Depending on the specific measurement campaign (T1-T5), the number of TLS stations ranged from 30 to 35. These were situated as shown in Fig. 4a. The points registered by the terrestrial laser scanner enabled the integration of the project and the development of a digital terrain model, which was obtained through parametric and algorithmic filtration processes.

3.2.3. Point cloud data filtering and DoD analysis

The next step involved point cloud processing to extract terrain points and generate a digital terrain model based on these data. A panoramic measurement of 360° enables automatic registration of scans via a multi-station adjustment method [49] in the RiSCAN PRO software version 2.9. It also allows the detection of reflectors that constitute the reference system for georeferencing the resulting LiDAR point cloud. Accurate alignment of the 3D GNSS scanner position, with the aid of IMU sensors and observations of reference targets, enables the precise reconstruction of a point cloud, which is subsequently subjected to post-processing to filter out terrain cover.

The resulting TLS data were filtered out, classified parametrically and processed algorithmically according to the methodology presented in [50]. The purpose was to extract class 2 data, which represents the ground (02 class ground LAS ASPRS). This procedure led to the removal of approximately 85% of the registered points. Automatic filtering out of low vegetation and manual extraction of features such as trees lying on the ground and leaves from the dataset posed the main challenge.

Differencing Digital Elevation Models is the prevalent technique for comparing point clouds in earth sciences, particularly applicable when the geometry of the scene is planar. In most cases, the raw collected data are gridded, to generate DEMs if the surface of the terrain is near horizontal [51]. The differential analysis of the models was performed on point clouds using the Cloud to Mesh distance method [40]. This study presents the results of the last (T5) TLS measurement campaign concerning the first surface (model T5-T1).

4. Results

4.1. Geodatabase of mining operation and differential analysis of ALS DEMs

Digitisation of 67 archival maps documenting mining operations in the "Pustków" field, produced a digital 3D reconstruction of underground workings. The resulting geodatabase was used for GIS-based analysis of spatial associations between identified discontinuous deformations and the locations of underground levels, shafts, drifts and declines. The preserved and available documentation is incomplete and does not present a complete overview of the past mining operations, as suggested by the subsidence basins and sinkholes visible on the ground's surface.

Differential analysis of two ALS DEMs (2011-2020) and their derivatives (slope and hill-shade surfaces) identified 83 potential sinkholes in the study area and 75 of these were confirmed as sinkholes during field investigation. These are marked in Fig. 3 representing the study area against the background of digitised mining plans together with 2 new sinkholes that emerged between 2011 and 2020 (marked in red). Information on these deformations was provided by the Lipinki Forestry Management. This specific area was subjected to shallow underground mining between 1964 and 1968 [52].

The depths of the identified sinkholes range from 0.85 to 4.8 m with the mean of 2.2 m, and the diameter ranges from 2.7 to 12.8 m with the mean of 5.6 m. Spatial analysis of sinkhole locations with the geodatabase of underground workings confirmed that the pair of new sinkholes formed directly above the shallow levels located up to 6-8 m below the terrain's surface. The larger sinkhole has been subjected to geodetic monitoring with terrestrial laser scanning.

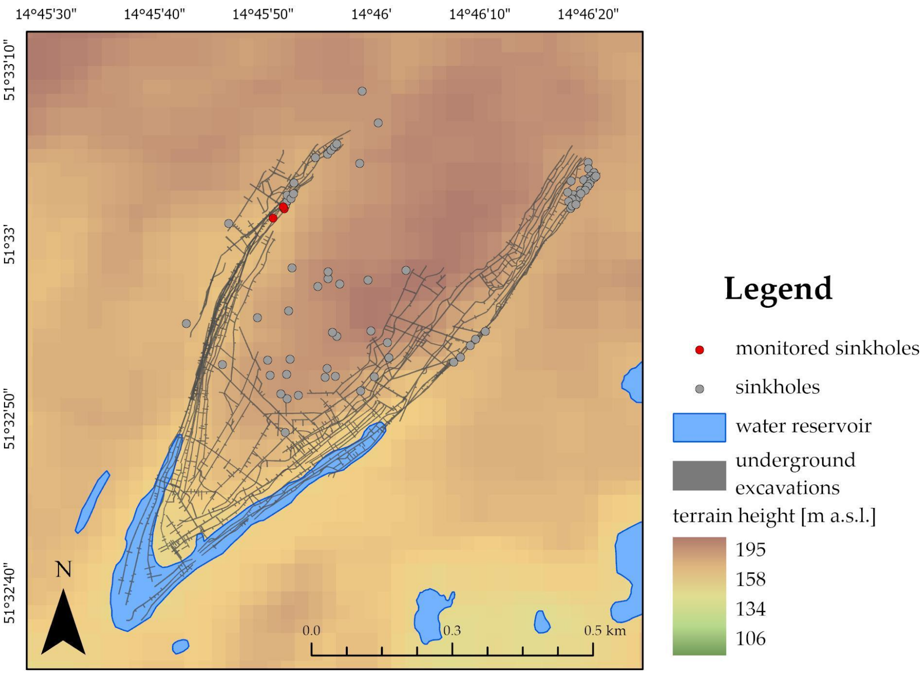

Fig. 3. Location of identified and monitored sinkholes in the underground mining study area

4.2. Results of TLS data processing

The centre points of reference targets set on the measurement control points were used as control points. No significant changes in the coordinates of the control points were detected between the T1 to T5 epochs. TABLE 1 contains the coordinates of control points used for point cloud georeferencing. Fig. 4a presents the configuration of the control network in the RiSCAN software and Fig. 4b is one of the TLS measurement stations and control point with a reference target placed on a bipod.

TABLE 1

Coordinates of control points for Epoch T1

Target No	X [m]	Y [m]	H [m]	mX; mY; mH [m]	Pole length (to the center of the target) [m]	H of the target center [m]
T1	5712911.84	5483672.19	148.157	0.006;0.015;0.016	2.160	150.317
T2	5712943.94	5483678.79	148.864	0.006;0.014;0.015	2.160	151.024
T3	5712940.75	5483643.51	149.589	0.005; 0.014; 0.015	2.160	151.759

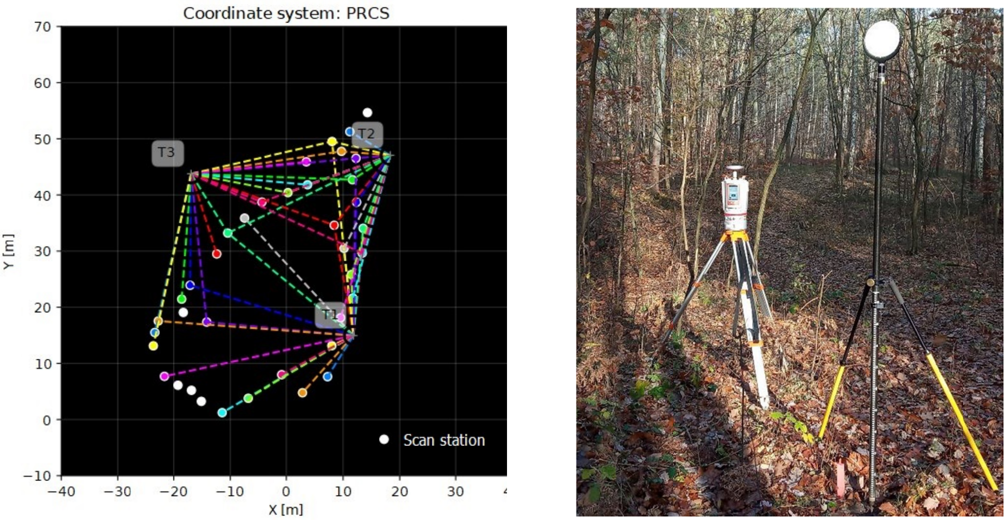

(a) (b)

Fig. 4. a) Plan of observations between scanner positions in PRCS (project coordinate system), b) identification of survey control point using TLS targets

Accuracy statistics for the TLS data fitted in the multi-station adjustment approach for epoch T5 are presented in TABLE 2.

TABLE 2

Deviations for the registered scanner positions using multi-station adjustment algorithms (epoch T5)

	dX [m]	dY [m]	dZ [m]
minimum deviation	–0.033	–0.036	–0.015
maximum deviation	0.032	0.034	0.011
average deviation	0.001	0.004	0.001
standard deviation	0.016	0.012	0.005
mean absolute deviation	0.016	0.008	0.003

Fig. 5a represents the TLS point cloud in RGB colours before filtration and Fig. 5b the same point cloud symbolised with reflectance intensity colours.

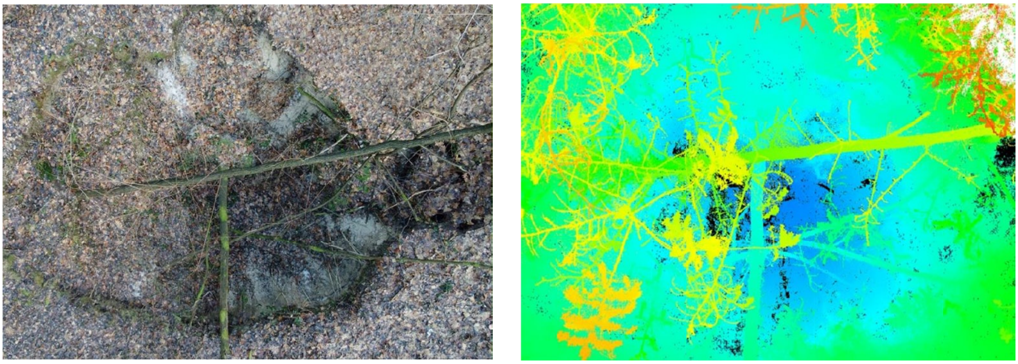

(a) (b)

Fig. 5. a) TLS point cloud before filtration in RGB colours, b) TLS point cloud seen in reflectance intensity colours

4.3. TLS monitoring

Up to the present date five TLS measurement campaigns (T1 to T5) were conducted, during the autumn and spring seasons to reduce the influence of vegetation. TABLE 3 contains the metadata of the datasets together with the accuracy statistics. Precise processing of the point cloud for each measurement period allowed for the development of a digital elevation model of the sinkhole area without vegetation. Based on the results of these measurements accurate dimensions of the analysed deformation feature were determined. These are 11.5 × 7 × 3.5 m in length/width/depth, respectively (Fig. 6).

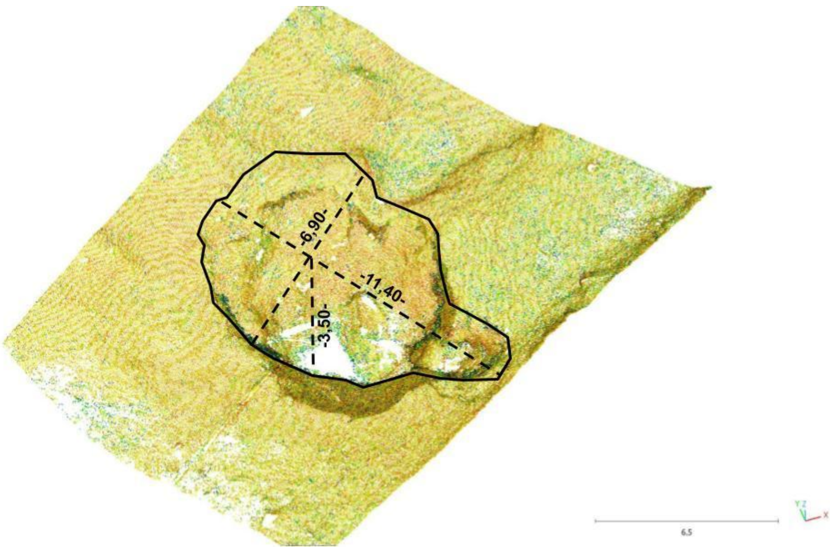

Fig. 6. 3D (isometric) view of the point cloud model of the sinkhole

The two-year monitoring was aimed at identifying the ground's surface changes inside the sinkhole and in its vicinity and analysinganalyse if there is any progress in the feature's dimensions.

TABLE 3

Acquisition dates and statistics for TLS data

Measurement Epoch	Date	Points / m^2	Vertical Accuracy [m]
T1	3.06.2020	200	≤0,03
T2	18.09.2020	220	≤0,03
T3	16.03.2021	210	≤0,03
T4	06.10.2021	200	≤0,03
T5	10.05.2022	220	≤0,03

The most straightforward way to compare two-point cloud data is by using the direct 3D point-to-point algorithm, which is the cloud-to-cloud distance [44]. The differential analyses were carried out using the Cloud-to-Mesh distance approach [53]. The MESH surface was the reference point cloud T1 presented in grayscale in Fig. 7a. The analysed point clouds were the T5

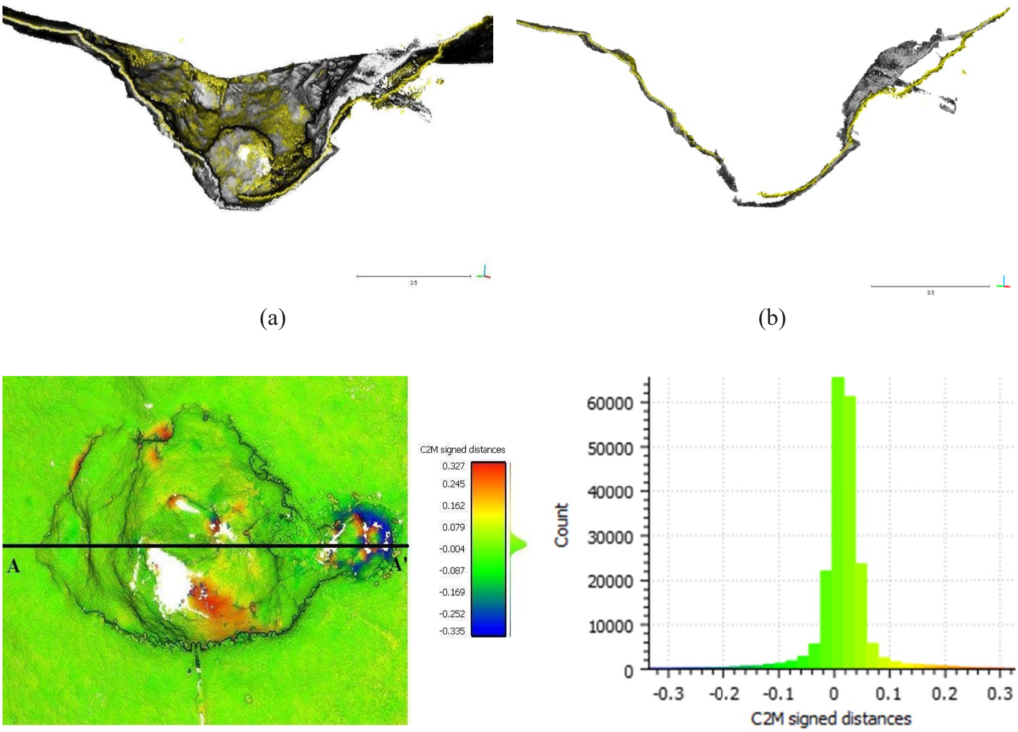

(a) (b)

(c) (d)

Fig. 7. (a) Visualization of a cross-section through the T1 TLS point cloud, (b) T5 data superimposed on T1 data, (c) DEM of difference (T1-T5), (d) histogram of distance differences between the point clouds T1-T5

data shown in yellow on the cross-section shown in Fig. 7b. The DEM of the difference between Cloud (T5) and Mesh (T1) as shown in Fig. 7c indicates that there is no progression in the depth of the sinkhole. However, an erosion process was detected. The material transported with rainwater flowing into the sinkhole on its western side accumulates at its bottom. This process causes a gradual retreat of the slope in this part of the sinkhole. The inflow of water towards the sinkhole can trigger further collapse due to its location above old shallow underground workings and possible water infiltration.

The histogram in Fig. 7d presents the differential distances between the two analysed surfaces. Approx. 90% of the data is between –10 to 10 cm, 5 % of the results represent distances less than –10 cm up to –30 cm and 5% of the total no of points is greater than 10 cm up to 33 cm.

5. Discussion and conclusions

The analysis of digital elevation models and their derivatives, developed from publicly available airborne laser scanning data, facilitates the detection of sinkholes and other types of ground surface deformations in post-mining areas. DEM of difference analysis of a minimum of two datasets allows for identifying deformations that developed between subsequent data acquisitions. The characteristics of the study area (particularly vegetation cover) prohibit the use of photogrammetry to register and study the development of sinkholes. The accuracy of point clouds registered with UAS or UAV LiDAR systems is not high enough [23] to detect small-scale changes in the shape of the analysed features in addition to insufficient temporal frequency of acquisition of publicly available data. Thus, the applied methodology based on a sequence of terrestrial laser scanning (TLS) measurements facilitated the documenting of recently discovered new sinkholes in a shallow underground post-mining area. Whereas, GIS-based digital reconstruction of old underground workings allowed for analysis of the feature spatial association with underground voids.

The two-year series of TLS measurements were conducted to inventory the new sinkhole and spatio-temporal analysis of potential further deformation processes. Analysis of differential TLS-based DEM indicated that the sinkhole has not undergone any further development. However, it also highlighted the occurrence of local erosion processes, which are related to the transport of loose material from the sinkhole slope by water and its deposition at the bottom. Terrestrial laser scanning allowed us to obtain a continuous 3D terrain model with small gaps on the bottom of the modelled sinkhole visible in Figs. 4 and 7c. It was caused by the scanner-look angle occlusion and obstruction of the LiDAR sensor beam.

The initial formation of the sinkhole can be explained by changes in groundwater conditions and the process of sediment movement into the post-mining void as a result of water infiltration and subsequent changes in saturation of the rock mass [54]. This indicates that continuous monitoring of ground surface movements and mapping subsidence risk zones is necessary in the post-mining area to mitigate risk associated with the sudden formation of new sinkholes in light of the ongoing tourist development of this part of the Muskau Arch Geopark.

The complex glaciotectonic geological composition of this area and the presence of various types of rocks in the overburden of coal seams (clays, silts, dry and saturated sands), make it challenging to predict the occurrence of such processes. Geodatabases documenting the location of old underground mining operations and geophysical prospecting confirming or locating underground voids and disturbed rock mass [55] can aid in identifying areas susceptible to potential sinkhole occurrence. To ensure up-to-date information, such post-mining areas should be subjected to periodic monitoring using low-altitude (UAV) or airborne laser scanning.

The results of this study, along with those described in other published works underline that discontinuous deformations can occur many years and decades after mining operations have ceased [30] and monitoring of post-mining areas should be treated as an eternal task [56]. During the course of 2 years of observations, it was verified that TLS is a highly effective and precise method for generating three-dimensional surface models. TLS, as an active measuring system, can process ground surfaces not concealed by vegetation for further analysis. The georeferencing of the TLS point cloud-based models on a stable control network is essential. The reference points are measured once a year using the total station technique and their location is set away from the sinkhole to minimise potential point movements while enabling accurate scanning of the targets during subsequent TLS campaigns. The limitation of this approach is the need for periodic in-situ measurements, which may prove difficult and hazardous, in remote or inaccessible locations in other post-mining sites.

Acknowledgements

This research was conducted as part of the National Science Centre's projects OPUS-17 t(2019/33/B/ST10/02975) and OPUS-22 (2021/43/B/ST10/02157) The authors would like to express their gratitude to Nadleśnictwo Lipinki – Lasy Państwowe for enabling the research within their forest district.

References

[1] W. Piwowarski, Modelling of discontinuous deformations over shallow post-mining voids in the rock mass. Acta Geodynamica et Geomaterialia, 253-256 (2019). DOI: https://doi.org/10.13168/AGG.2019.0021

[2] J.N. Van Der Merwe, The development of a time-based probabilistic sinkhole prediction method for coal mining in the Witbank and Highveld coalfields. J. S. Afr. Inst. Min. Metall. **120**, 6, 393-398 (2020).

[3] P. Strzałkowski, The influence of selected mining and natural factors on the sinkhole creation hazard based on the case study. Environmental Earth Sciences **80**, 117 (2021). DOI: https://doi.org/10.1007/s12665-021-09403-1

[4] R. Ścigała, K. Szafulera, M. Jendryś, Assessment of sinkhole hazard in the post-mining area using the ERT method and numerical modeling. Scientific Journals of the Maritime University of Szczecin, Zeszyty Naukowe Akademii Morskiej w Szczecinie **75** (147), 20-34 (2023).

[5] H. Kratzsch, Mining Subsidence Engineering. Springer-Verlag Berlin Heidelberg New York (1983).

[6] K. Tajduś, A. Sroka, R. Misa, M. Dudek, Przykłady zagrożeń powierzchni terenu deformacjami nieciągłymi typu powierzchniowego ujawniające się nad zlikwidowanymi podziemnymi wyrobiskami górniczymi. Prace Instytutu Mechaniki Górotworu PAN **19**,3, 3-10 (2017).

[7] O. Kaszowska, A. Kowalski, Wpływ podziemnej eksploatacji górniczej na powierzchnię terenu. Przegląd Geologiczny **55**, 8, 640-641 (2007).

[8] J.K. Pringle, et al., Geophysical characterization of derelict coalmine workings and mineshaft detection: a case study from Shrewsbury, United Kingdom. Near Surface Geophysics **6**, 185-194 (2008). DOI: https://doi.org/10.3997/1873-0604.2008014

[9] Z. Pilecki, E. Popiołek, Geodezyjne i geofizyczne rozpoznanie zagrożenia zapadliskowego. Bezpieczeństwo Pracy i Ochrona Środowiska w Górnictwie **6**(190), 34-39 (2010).

[10] Z. Pilecki, et al., Identification of buried historical mineshaft using ground-penetrating radar. Engineering Geology **294**, 106400 (2021). DOI: https://doi.org/10.1016/j.enggeo.2021.106400

[11] J. Maciaszek, System informacji o archiwalnych mapach i polach górniczych na potrzeby zagospodarowania przestrzennego. Wydawnictwa AGH, Kraków (2010).

[12] J. Blachowski, W. Milczarek, P. Stefaniak, Deformation information system for facilitating studies of mining-ground deformations, development, and applications. NHESS **14**,7, 1677-1689 (2014). DOI: https://doi.org/10.5194/nhess-14-1677-2014

[13] A. Gontaszewska, Podziemna eksploatacja węgla brunatnego na Ziemi Lubuskiej – dawne górnictwo, współczesny problem. Przegląd Górniczy **71**, 10, 1-8 (2015).

[14] I. Contrucci et al., Aseismic Mining Subsidence in an Abandoned Mine: Influence Factors and Consequences for Post-Mining Risk Management. Pure Appl. Geophys. **176**, 801-825 (2019). DOI: https://doi.org/10.1007/s00024-018-2015-6

[15] H.J. Oh, S. Lee, Assessment of ground subsidence using GIS and the weights-of-evidence model. Engineering Geology **115**, 36-48 (2010). DOI: https://doi.org/10.1016/j.enggeo.2010.06.015

[16] S. Lee, Y. Park, Application of decision tree model for the ground subsidence hazard mapping near abandoned underground coal mines. Journal of Environmental Management **127**, 166-176 (2013). DOI: https://doi.org/10.1016/j.jenvman.2013.04.010

[17] A. Sroka, K. Tajduś, R. Misa, M. Clostermann, The possibility of discontinuity/sinkholes appearance with the determination of their geometry in the case of shallow drifts. Mat. 18. ALTBERGBAU – KOLLOQUIUM Wieliczka (2018).

[18] P. Strzałkowski, Sinkhole formation hazard assessment. Environmental Earth Sciences **78**, 9, 1-6 (2019). DOI: https://doi.org/10.1007/s12665-018-8002-5

[19] Górnośląski System Informacji o Zagrożeniach Powierzchni na Terenach Zlikwidowanych Kopalń. https://zapadliska.gig.eu/, accessed: 10-07-2023.

[20] F. Gutiérrez et al., Review on sinkhole monitoring and performance of remediation measures by high precision leveling and terrestrial laser scanner in the salt karst of the Ebro Valley, Spain. Engineering Geology **248**, 283-308 (2019). DOI: https://doi.org/10.1016/j.enggeo.2018.12.004

[21] J. Sevil, A. Benito-Calvo, F. Gutiérrez, Sinkhole subsidence monitoring combining terrestrial laser scanner and high-precision levelling. Earth Surface Processes and Landforms **46**, 8, 1431-1444 (2021). DOI: https://doi.org/10.1002/esp.5112

[22] J. Suh, Y. Choi, Mapping hazardous mining-induced sinkhole subsidence using unmanned aerial vehicle (drone) photogrammetry. Environmental Earth Sciences 76 (2017). DOI: https://doi.org/10.1007/s12665-017-6458-3

[23] G. Jóźków, A. Walicka, A. Borkowski, Monitoring Terrain Deformations Caused by Underground Mining Using UAV Data. The International Archives of Photogrammetry, Remote Sensing and Spatial Information Sciences **43**, 737-744 (2021). DOI: https://doi.org/10.5194/isprs-archives-XLIII-B2-2021-737-2021

[24] E. Intrieri, Sinkhole monitoring and early warning: An experimental and successful GB-InSAR application. Geomorphology **241**, 304-314 (2015). DOI: https://doi.org/10.1016/j.geomorph.2015.04.018

[25] O. Orhan, M. Yakar, S. Ekercin, An application on sinkhole susceptibility mapping by integrating remote sensing and geographic information systems. Arabian Journal of Geosciences **13** (17), 1-17 (2020). DOI: https://doi.org/10.1007/s12517-020-05841-6

[26] A. Malinowska, et al., Sinkhole occurrence monitoring over shallow abandoned coal mines with satellite-based persistent scatterer interferometry. Engineering Geology **262**, 105336 (2019). DOI: https://doi.org/10.1016/j.enggeo.2019.105336

[27] Państwowy Instytut Geologiczny – Państwowy Instytut Badawczy, Raport drugi z prac analitycznych o deformacjach terenu w TrzebinI, (praca zbiorowa), (2023).

[28] J. Koźma, M. Kupetz, The transboundary Geopark Muskau Arch (Geopark Łuk Mużakowa, Geopark Muskauer Faltenbogen). Przegląd Geologiczny **56**, 8/1, 692-698 (2008).

[29] J. Badura et al., Geopark "Łuk Mużakowa" – proponowany transgraniczny obszar ochrony georóżnorodności, Przegląd Geologiczny **51**, 54-58 (2003).

[30] A. Gontaszewska, Szkody górnicze, W: A. Greinert (red.) Wydobycie węgla brunatnego i rekultywacja terenów pokopalnianych w regionie lubuskim. Uniwersytet Zielonogórski, Zielona Góra, 146-157 (2015).

[31] J. Koźma, Antropogeniczne zmiany krajobrazu związane z dawnym górnictwem węgla brunatnego na przykładzie polskiej części obszaru łuku Mużakowa. Górnictwo Odkrywkowe **57**, 3, 5-13 (2016).

[32] T. Chrzan, Wpływ wydobycia węgla brunatnego na środowisko naturalne w Łuku Mużakowskim. Zeszyty Naukowe Politechniki Śląskiej **243**, 1436, 29-34 (1999).

[33] H. Greinert, M. Drab, A. Greinert, Studia nad efektywnością leśnej rekultywacji zwałowisk fitotoksycznie kwaśnych piasków mioceńskich po byłej kopalni węgla brunatnego w Łęknicy. Oficyna Wydawnicza Uniwersytetu Zielonogórskiego, Zielona Góra (2009).

[34] K. Świerkosz, J. Koźma, K. Reczyńska, M. Halama, Muskau Arch Geopark in Poland (Central Europe) – Is it Possible to Integrate Geoconservation and Geoeducation into Biodiversity Conservation? Geoheritage, (2016), DOI: https://doi.org/10.1007/s12371-016-0178-z

[35] K. Labus, S. Skoczyńska, Origin of sulphates in post-mining lakes in the eastern part of the Muskau Arch (Polish–German borderland). Geological Quarterly **57** (3), 561-566 (2013). DOI: http://dx.doi.org/10.7306/gq.1110

[36] M. Gąsiorowski, J. Stienss, E. Sienkiewicz, I. Sekudewicz, Geochemical Variability of Surface Sediment in Post-Mining Lakes Located in the Muskau Arch (Poland) and Its Relation to Water Chemistry. Water Air Soil Pollut, **232**, 108 (2021). DOI: https://doi.org/10.1007/s11270-021-05057-8

[37] M. Oszkinis-Golon, M. Frankowski, A. Pukacz, Macrophyte Diversity as a Response to Extreme Conditions in the Post-Mining Lakes of the Muskau Arch (West Poland). Water **13**, 2909 (2021). DOI: https://doi.org/10.3390/w13202909

[38] A. Gontaszewska, A. Kraiński, Deformacje powierzchni terenu na obszarze dawnego podziemnego górnictwa węgla brunatnego w okolicy Zielonej Góry. W: Wybrane problemy badań geologicznych i hydrogeologicznych dla górnictwa i energetyki. Wyd. GIG, Katowice, 108-119, (2012).

[39] U. Münch, P. Nestler, Airborne Laserscanning als Ergänzung der Erkundungsmethoden von Braunkohlen-Altbergbau – Airborne Laserscanning, an additional technique for evaluation of hazards caused by underground lignite mining, Brandenburgische Geowissenschaftliche Beiträge **10**, 1/2, 7-18 (2003).

[40] D. Lague, N. Brodu, J. Leroux, Accurate 3D comparison of complex topography with terrestrial laser scanner: Application to the Rangitikei canyon (NZ). ISPRS Journal of Photogrammetry and Remote Sensing **82**, 10-26 (2013). DOI: https://doi.org/10.1016/j.isprsjprs.2013.04.009

[41] R. D. Williams, DEMs of Difference. Geomorphological Techniques, Chap. 2, Sec. 3.2 (2012).

[42] A. Yalcin, F. Bulut, Landslide susceptibility mapping using GIS and digital photogrammetric techniques: a case study from Ardesen (NE-Turkey). Natural Hazards **41**, 1, 201-226 (2007). DOI: https://doi.org/10.1007/s11069-006-9030-0

[43] M. Eeckhaut et al., Use of LIDAR-derived images for mapping old landslides under forest. Earth Surface Processes and Landforms **32**, 5, 754-769 (2007). DOI: https://doi.org/10.1002/esp.1417

[44] D. Girardeau-Montaut, M. Roux, R. Marc, G. Thibault, Change detection on points cloud data acquired with a ground laser scanner. International Archives of Photogrammetry, Remote Sensing and Spatial Information Sciences **36**, 3, 30-35, (2005).

[45] O. Monserrat, M. Crosetto, Deformation measurement using terrestrial laser scanning data and least squares 3D surface matching. ISPRS Journal of Photogrammetry and Remote Sensing **63**, 1, 142-154 (2008). DOI: https://doi.org/10.1016/j.isprsjprs.2007.07.008

[46] M. Kazhdan, M. Bolitho, H. Hoppe, Poisson Surface Reconstruction. In: Proc. of the 4th Eurographics Symposium on Geometry Processing, 61-70 (2006). DOI: https://doi.org/10.2312/SGP/SGP06/061-070

[47] Z. Dong, et al., Registration of large-scale terrestrial laser scanner point clouds: A review and benchmark. ISPRS Journal of Photogrammetry and Remote Sensing **163**, 327-342 (2020). DOI: https://doi.org/10.1016/j.isprsjprs.2020.03.013

[48] Riegl Data Measurement System, Riegl VZ-400i. http://www.riegl.com/uploads/tx_pxpriegldownloads/RIEGL_VZ-400i_Datasheet_2022-09-27.pdf, accessed: 10-07-2023.

[49] P. Wilkes, A. Lau, M. Disney, K. Calders, A. Burt, J.G. de Tanago, H. Bartholomeus, B. Brede, M. Herold, Data acquisition considerations for terrestrial laser scanning of forest plots. Remote Sensing of Environment **196**, 140-153 (2017). DOI: https://doi.org/10.1016/j.rse.2017.04.030

[50] P. Axelsson, Processing of laser scanner data – algorithms and applications. ISPRS Journal of Photogrammetry and Remote Sensing **54**, 2-3, 138-147 (1999). DOI: https://doi.org/10.1016/S0924-2716(99)00008-8

[51] S. Lane, N. Richard, M. Westaway, D. Murray Hicks, Estimation of erosion and deposition volumes in a large, gravel-bed, braided river using synoptic remote sensing. Earth surface processes and landforms: the journal of the British Geomorphological Research Group 28.3, p. 249-271 (2003). DOI: https://doi.org/10.1002/esp.483

[52] J. Koźma, Geoturystyczne walory krajobrazu Łuku Mużakowa. Górnictwo Odkrywkowe **3**, 32-40 (2017).

[53] P. Cignoni, C. Rocchini, R. Scopigno, Metro: measuring error on simplified surfaces. Computer graphics forum. Vol. 17. No. 2. Oxford, UK and Boston, USA: Blackwell Publishers (1998). DOI: https://doi.org/10.1111/1467-8659.00236

[54] A. Malinowska, A. Matonóg, Sinkhole hazard maping with the use of spatial analysis and analytical hierarchy process in the light of mining-geological factors. Acta Geodyn. Geomater. **14**, 2 (186), 159-172 (2017). DOI: https://doi.org/10.13168/AGG.2016.0037

[55] J. Blachowski, E. Warchala, J. Koźma, A. Buczyńska, N. Bugajska, M. Becker, D. Janicki, P. Kujawa, L. Kwaśny, J. Wajs, et al., Geophysical Research of Secondary Deformations in the Post Mining Area of the Glaciotectonic Muskau Arch Geopark – Preliminary Results. Applied Sciences. **12** (3), 1194 (2022). DOI: https://doi.org/10.3390/app12031194

[56] J. Kretschmann, N. Nguyen, Research Areas in Post-Mining – Experiences from German Hard Coal Mining. J. Pol. Miner. Eng. Soc. **1**, 255-262 (2020). DOI: https://doi.org/10.29227/IM-2020-02-31